

## Study on the mixed crystals $(\text{NH}_4)_{2-x}\text{K}_x\text{SO}_4$

This article has been downloaded from IOPscience. Please scroll down to see the full text article.

1997 J. Phys.: Condens. Matter 9 2657

(<http://iopscience.iop.org/0953-8984/9/12/012>)

View [the table of contents for this issue](#), or go to the [journal homepage](#) for more

Download details:

IP Address: 171.66.16.151

The article was downloaded on 12/05/2010 at 23:07

Please note that [terms and conditions apply](#).

## Study on the mixed crystals $(\text{NH}_4)_{2-x}\text{K}_x\text{SO}_4$

C González-Silgo<sup>†</sup>, X Solans<sup>‡</sup>, C Ruiz-Pérez<sup>†</sup>, M L Martínez-Sarrión<sup>§</sup>,  
L Mestres<sup>§</sup> and E Bocanegra<sup>||</sup>

<sup>†</sup> Departamento Física Fundamental y Experimental, Universidad de la Laguna, E-38204-La Laguna, Spain

<sup>‡</sup> Departamento Cristallografia, Mineralogia i Dipòsits Minerals, Universitat de Barcelona, E-08028-Barcelona, Spain

<sup>§</sup> Departamento Química Inorgànica, Universitat de Barcelona, E-08028-Barcelona, Spain

<sup>||</sup> Departamento Física Aplicada II, Universidad del Pais Vasco, E-48080-Bilbao, Spain

Received 10 September 1996, in final form 18 November 1996

**Abstract.** A study on the mixed crystals of formula  $(\text{NH}_4)_{2-x}\text{K}_x\text{SO}_4$  ( $1 > x > 0$ ) has been carried out, using thermal analyses and x-ray diffraction on powder and single-crystal samples at different temperatures. It is shown that mixed crystals with  $x < 0.34$  have a transition from the paraelectric to the ferroelectric phase;  $T_c$  decreases as the value of  $x$  increases. The orientation of the sulphate ion with respect to the crystallographic axes depends on the value of  $x$ . Mixed crystals with the paraelectric–ferroelectric transition turn around the  $b$  axis when the temperature decreases in the paraelectric phase, while in mixed crystals without a transition the orientation of the sulphate ion does not alter when the temperature varies. The transition is displacive, increasing the value of the parameter  $a$  without a soft mode. This is deduced from a study of the crystal structures, the translational and libration tensors and a density map of the sum of the bond valences.

### 1. Introduction

Ammonium sulphate undergoes a phase transition at  $T_c = 223.5$  K [1]. In the paraelectric phase, above  $T_c$ , the crystal is orthorhombic with the space group Pnam. At  $T_c$  the crystal transforms to Pna2<sub>1</sub> and spontaneous polarization appears along the  $c$  axis. Well known thermal analysis and dielectric measurements on  $(\text{NH}_4)_2\text{SO}_4$  were carried out by Hoshino *et al* [2].

The peculiar properties of the phase transition of  $(\text{NH}_4)_2\text{SO}_4$  has been explained by two phenomenological theories: a ferrielectric model with two order parameters based upon a sublattice model and assuming an order–disorder transition [3, 4] and an improper or pseudo-proper model with some displacive order parameter according to the dynamic behaviour of a soft mode [5]. The first theory does not agree with the thermal analysis on the deuterated compound [2], while Raman spectroscopy [6] and NMR [7] measurements suggest that a soft mode is not produced during the phase transition.

The mixed crystals  $(\text{NH}_4)_{2-x}\text{K}_x\text{SO}_4$  have been studied by several workers. Sawada *et al* [8], from the temperature dependence of the spontaneous polarization in the mixed crystals, suggested that the substitutions are not equivalent in the two crystallographic ammonium sites. Kasahara *et al* [9], from a study on the spin–lattice relaxation time of protons, reported that more potassium ions are substituted for ammonium ions on the site K(1) (potassium ion coordinated to 11 oxygen atoms). This result was corroborated by Shiozaki *et al* [10] by x-ray diffraction on single crystals of  $(\text{NH}_4)_{1.37}\text{K}_{0.63}\text{SO}_4$  and  $(\text{NH}_4)_{0.6}\text{K}_{1.4}\text{SO}_4$ .

**Table 1.** Crystal data and refinement. Coincident values are given only in the first column.  
 $R = \Sigma \|F_o\| - |F_c| / \Sigma \|F_o\|$ ;  $wR = \Sigma w \|F_o\|^2 - |F_c|^2 / \Sigma w \|F_o\|^2$ .

<i>x</i>	0	1.90	1.90	1.90
Temperature (K)	231.5(5)	298.3(1)	234.6(5)	174.8(9)
Formula weight	132.14	172.09	172.09	172.09
Wavelength (Å)	0.71069			
Crystal system	Orthorhombic			
Space group	Pnam			
<i>a</i> (Å)	7.733(2)	7.5000(9)	7.4835(10)	7.4691(12)
<i>b</i> (Å)	10.588(3)	10.0755(14)	10.063(2)	10.028(2)
<i>c</i> (Å)	5.992(4)	5.790(3)	5.778(3)	5.796(5)
Volume (Å <sup>3</sup> )	490.6(4)	437.5(2)	435.1(2)	434.1(4)
<i>Z</i>	4			
$\rho_x$ (Mg m <sup>-3</sup> )	1.789	2.613	2.627	2.633
$\mu$ (mm <sup>-1</sup> )	0.576	2.428	2.442	2.447
<i>F</i> (000)	280	341	341	341
Crystal size (mm × mm × mm)	0.2 × 0.2 × 0.3	0.2 × 0.1 × 0.1	0.2 × 0.1 × 0.1	0.2 × 0.1 × 0.1
$\theta$ range for data (°)	3.3–29.9	3.4–30.0	3.4–30.0	3.4–30.0
Index ranges	0 ≤ <i>h</i> ≤ 10 0 ≤ <i>k</i> ≤ 14 0 ≤ <i>l</i> ≤ 8			
Number of reflections collected	778	706	702	778
Number of independent reflections	778	699	695	778
Number of data; number of parameters	728; 61	678; 42	672; 42	586; 43
Goodness of fit on <i>F</i> <sup>2</sup>	0.820	1.129	0.953	0.821
Final <i>R</i> (observed)	0.031	0.031	0.0275	0.0982
Final <i>wR</i> (observed)	0.081	0.0786	0.0727	0.2914
Extinction coefficient	0.130(14)	0.038(5)	0.047(6)	0.1(2)
Largest difference peak (electrons Å <sup>-3</sup> )	0.465	0.711	0.520	0.764
Largest difference hole (electrons Å <sup>-3</sup> )	−0.412	−0.706	−0.796	−0.817
<i>x</i>	0.20	0.20	0.20	
Temperature (K)	298.3(1)	232.8(4)	183.8(9)	
Formula weight	136.94	136.94	136.94	
Wavelength (Å)	0.71069			
Crystal system	Orthorhombic			
Space group	Pnam	Pnam	Pna21	
<i>a</i> (Å)	7.747(2)	7.7230(14)	7.7834(13)	
<i>b</i> (Å)	10.561(5)	10.542(6)	10.514(5)	
<i>c</i> (Å)	5.9463(11)	5.931(2)	5.9090(12)	
Volume (Å <sup>3</sup> )	486.5(3)	482.7(3)	483.6(3)	
<i>Z</i>	4			
$\rho_x$ (Mg m <sup>-3</sup> )	1.870	1.890	1.881	
$\mu$ (mm <sup>-1</sup> )	0.773	0.777	0.778	
<i>F</i> (000)	287			
Crystal size (mm × mm × mm)	0.2 × 0.1 × 0.1			
$\theta$ range for data (°)	3.3–29.9			
Index ranges	0 ≤ <i>h</i> ≤ 10 0 ≤ <i>k</i> ≤ 14 0 ≤ <i>l</i> ≤ 8			
Number of reflections collected	776	771	763	
Number of independent reflections	769	764	763	
Number of data; number of parameters	719; 63	714; 63	713; 95	
Goodness of fit on <i>F</i> <sup>2</sup>	1.106	1.090	1.009	
Final <i>R</i> ( <i>I</i> > 2σ( <i>I</i> ))	0.0259	0.0254	0.0219	
Final <i>wR</i> ( <i>I</i> > 2σ( <i>I</i> ))	0.0664	0.0689	0.0554	
Extinction coefficient	0.060(7)	0.100(10)	0.069(7)	
Largest difference peak (electrons Å <sup>-3</sup> )	0.356	0.521	0.527	
Largest difference hole (electrons Å <sup>-3</sup> )	−0.270	−0.332	−0.210	

**Table 2.** Final atomic coordinates ( $\times 10^4$ ; hydrogen atoms  $\times 10^3$ ) and anisotropic thermal coefficients ( $\times 10^3$ ). X = N and K.

	$x/a$	$y/b$	$z/c$	$U_{11}$	$U_{22}$	$U_{33}$	$U_{23}$	$U_{13}$	$U_{12}$
$x = 0; T = 231.5$ K									
S	2456(1)	4195(1)	2500	14(1)	16(1)	19(1)	0	0	0(1)
N(1)	1902(2)	981(1)	2500	20(1)	24(1)	24(1)	0	0	0(1)
N(2)	-341(2)	7035(1)	2500	25(1)	26(1)	26(1)	0	0	-3(1)
O(1)	3263(1)	3674(1)	482(2)	40(1)	31(1)	31(1)	-14(1)	8(1)	7(1)
O(2)	624(2)	3872(2)	2500	14(1)	58(1)	58(1)	0	0	-13(1)
O(3)	2684(2)	5571(2)	2500	43(1)	49(1)	49(1)	0	0	-2(1)
H(11)	283(5)	126(4)	250	47(8)					
H(12)	123(5)	156(4)	250	47(8)					
H(13)	174(5)	52(3)	353(5)	87(10)					
H(21)	59(4)	652(3)	250	39(7)					
H(22)	-21(4)	783(4)	250	45(7)					
H(23)	-99(4)	690(3)	367(6)	73(8)					
$x = 0.20; T = 298.3$ K									
S	2425(1)	4193(1)	2500	19(1)	21(1)	22(1)	0	0	0(1)
O(1)	3206(1)	3640(1)	476(2)	51(1)	50(1)	33(1)	-12(1)	9(1)	10(1)
O(2)	582(2)	3931(2)	2500	22(1)	78(1)	62(1)	0	0	-15(1)
O(3)	2741(2)	5570(1)	2500	54(1)	22(1)	52(1)	0	0	-5(1)
X(1)	1875(2)	861(1)	2500	24(1)	26(1)	27(1)	0	0	1(1)
X(2)	-268(1)	7071(1)	2500	26(1)	29(1)	30(1)	0	0	-1(1)
H(11)	281(6)	127(4)	250	81(13)					
H(12)	133(5)	149(4)	250	61(9)					
H(13)	166(6)	42(4)	358(7)	135(14)					
H(21)	-23(5)	767(5)	250	52(10)					
H(22)	78(7)	655(5)	250	98(15)					
H(23)	-106(4)	693(3)	151(5)	76(8)					
$x = 0.20; T = 232.8$ K									
S	2422(1)	4195(1)	2500	11(1)	19(1)	19(1)	0	0	0(1)
O(1)	3222(1)	3649(1)	471(2)	34(1)	46(1)	30(1)	-12(1)	8(1)	7(1)
O(2)	586(2)	3919(2)	2500	13(1)	65(1)	52(1)	0	0	-12(1)
O(3)	2728(2)	5579(1)	2500	33(1)	21(1)	45(1)	0	0	-3(1)
X(1)	1875(1)	971(1)	2500	14(1)	24(1)	21(1)	0	0	0(1)
X(2)	-285(1)	7063(1)	2500	16(1)	25(1)	23(1)	0	0	-1(1)
H(11)	277(8)	119(5)	250	75(15)					
H(12)	123(7)	144(5)	250	67(14)					
H(13)	169(4)	55(3)	353(6)	74(11)					
H(21)	-12(4)	767(4)	250	29(9)					
H(22)	73(6)	644(3)	250	47(10)					
H(23)	-79(5)	691(3)	150(5)	60(9)					

Martínez-Sarrión *et al* [11] studied mixed crystals with the formula  $(NH_4)_xM_{2-x}SO_4$ , where  $M = Na^+, Li^+, Rb^+$  or  $Tl^+$ , and showed the existence and the dependence of the transition temperature on the value of  $x$  and the ion size. Martínez-Sarrión *et al* [12] and González-Silgo *et al* [13] studied the mixed crystals  $(NH_4)_2(SO_4)_x(SeO_4)_{1-x}$  and  $(NH_4)_2(SO_4)_x(BeF_4)_{1-x}$ , respectively. The substitution of sulphate by selenate causes an increase in the Curie point and the fluoroberyllate anion produces a delay in the transition temperature of the second compound.

In this paper we attempt to obtain more information about the substitution of potassium and ammonium and about the structural transition mechanism. In particular the role of the hydrogen bond combined with the rotation of the sulphate anions is studied, to confirm

Table 2. (Continued)

	$x/a$	$y/b$	$z/c$	$U_{11}$	$U_{22}$	$U_{33}$	$U_{23}$	$U_{13}$	$U_{12}$
$x = 0.20; T = 183.8 \text{ K}$									
S	2413(1)	4210(1)	2410(1)	12(1)	15(1)	14(1)	-1(1)	1(1)	-1(1)
O(4)	3008(2)	3774(2)	4665(3)	29(1)	24(1)	17(1)	4(1)	-4(1)	2(1)
O(1)	3313(2)	3486(1)	637(3)	30(1)	24(1)	22(1)	-7(1)	8(1)	2(1)
O(2)	566(2)	4004(2)	2209(4)	13(1)	40(1)	36(1)	-2(1)	-2(1)	-7(1)
O(3)	2821(2)	5585(1)	2162(3)	24(1)	15(1)	23(1)	1(1)	0(1)	-2(1)
X(1)	1819(2)	1002(1)	2392(3)	16(1)	18(1)	16(1)	1(1)	0(1)	-1(1)
X(2)	-218(1)	7031(1)	2432(3)	15(1)	19(1)	18(1)	0	0	1(1)
H(11)	87(6)	140(4)	201(9)	54(11)					
H(12)	187(5)	91(3)	378(8)	28(8)					
H(13)	265(4)	151(4)	191(7)	28(8)					
H(14)	233(10)	25(10)	233(40)	168(37)					
H(21)	-20(4)	774(3)	260(9)	25(7)					
H(22)	-50(7)	684(5)	381(10)	50(13)					
H(23)	53(7)	663(5)	235(14)	60(13)					
H(24)	-102(5)	677(4)	140(7)	30(9)					
$x = 1.90; T = 298.3 \text{ K}$									
S	2337(1)	4198(1)	2500	12(1)	20(1)	13(1)	0	0	-1(1)
O(1)	3029(2)	3527(1)	417(2)	33(1)	33(1)	19(1)	-6(1)	4(1)	7(1)
O(2)	390(2)	4151(2)	2500	12(1)	45(1)	39(1)	0	0	-5(1)
O(3)	2953(2)	5589(2)	2500	24(1)	21(1)	30(1)	0	0	-5(1)
X(1)	1750(1)	897(1)	2500	19(1)	31(1)	20(1)	0	0	1(1)
K(2)	-119(1)	7044(1)	2500	15(1)	26(1)	21(1)	0	0	0(1)
$x = 1.90; T = 234.6 \text{ K}$									
S	2334(1)	4198(1)	2500	9(1)	18(1)	10(1)	0	0	0(1)
O(1)	3032(2)	3527(1)	407(2)	26(1)	29(1)	15(1)	-5(1)	4(1)	5(1)
O(2)	386(2)	4152(2)	2500	09(1)	39(1)	32(1)	0	0	-4(1)
O(3)	2960(2)	5592(2)	2500	21(1)	20(1)	23(1)	0	0	-4(1)
X(1)	1742(1)	897(1)	2500	16(1)	27(1)	15(1)	0	0	1(1)
K(2)	-121(1)	7039(1)	2500	12(1)	23(1)	16(1)	0	0	0(1)
$x = 1.90; T = 174.8 \text{ K}$									
S	2456(1)	4194(1)	2500	9(1)	10(1)	14(1)	0	0	0(1)
O(1)	3265(5)	3672(4)	481(7)	32(2)	36(2)	22(2)	-14(1)	7(1)	7(1)
O(2)	638(7)	3866(7)	2500	11(2)	48(3)	47(3)	0	0	-13(2)
O(3)	2691(9)	5563(6)	2500	36(3)	9(2)	40(3)	0	0	0(2)
X(1)	1896(7)	981(5)	2500	69(3)	68(2)	70(3)	0	0	-1(2)
K(2)	-345(7)	7025(5)	2500	73(2)	70(2)	78(2)	0	0	-1(2)

a displacive transition which is not driven typically by soft modes. The possibilities of disorder in the ammonium ions, as has been suggested, will be discussed.

## 2. Experimental section

### 2.1. Synthesis

The  $(\text{NH}_4)_2\text{SO}_4$  and  $\text{K}_2\text{SO}_4$  starting materials were of analytical reagent grade. Mixed crystals of general formula  $(\text{NH}_4)_{2-x}\text{K}_x\text{SO}_4$  ( $1 > x > 0$ ) were obtained by mixing  $(\text{NH}_4)_2\text{SO}_4$  and  $\text{K}_2\text{SO}_4$  in different ratios in an aqueous solution and thermostating at 313 K. Crystals were obtained by the slow evaporation method. The value of  $x$  for the powder

**Table 3.** Intra-ionic bond lengths and angles. O(4) = O(1'); H(14) = H(13') and H(24) = H(23') for paraelectric phases.

	Bond length (Å)						
	x = 0		x = 0.20		x = 1.90		
	231.8 K	298.3 K	232.8 K	183.8 K	298.3 K	234.6 K	174.8 K
S–O(1)	1.4687(12)	1.4679(9)	1.466(2)	1.483(2)	1.4771(13)	1.4801(13)	1.418(3)
S–O(2)	1.4572(14)	1.454(13)	1.457(2)	1.4585(13)	1.461(2)	1.459(2)	1.39 7(5)
S–O(3)	1.467(2)	1.475(2)	1.477(2)	1.487(2)	1.475(2)	1.478(2)	1.384(6)
S–O(4)	1.4687(12)	1.4679(9)	1.466(2)	1.472(2)	1.4771(13)	1.4801(13)	1.418(3)
N(1)–H(11)	0.78(5)	0.79(5)	0.77(7)	0.98(2)			
N(1)–H(12)	0.80(4)	0.69(4)	0.69(8)	1.01(2)			
N(1)–H(13)	0.80(4)	0.87(4)	0.78(4)	1.03(2)			
N(1)–H(14)	0.80(4)	0.87(4)	0.78(4)	0.98(4)			
N(2)–H(21)	0.90(5)	0.98(6)	1.00(6)	1.00(2)			
N(2)–H(22)	0.85(5)	0.63(5)	0.72(8)	0.98(2)			
N(2)–H(23)	0.87(4)	0.86(3)	0.74(4)	0.99(3)			
N(2)–H(24)	0.87(4)	0.86(3)	0.74(4)	1.00(3)			

	Bond angle (°)						
	x = 0		x = 0.20		x = 1.90		
	298.3 K	298.3 K	232.8 K	183.8 K	298.3 K	234.6 K	174.8 K
O(2)–S–O(3)	110.48(10)	110.49(10)	110.45(13)	110.27(9)	110.13(11)	110.29(11)	110.9(4)
O(2)–S–O(1)	108.96(6)	109.22(6)	109.16(9)	109.54(12)	109.67(7)	109.73(7)	109.1(2)
O(3)–S–O(1)	108.79(6)	108.89(6)	108.90(7)	109.31(10)	108.93(7)	108.74(7)	108.2(2)
O(2)–S–O(4)	108.96(6)	109.22(6)	109.16(9)	109.60(12)	109.67(7)	109.73(7)	109.1(2)
O(3)–S–O(4)	108.79(6)	108.89(6)	108.90(7)	108.77(10)	108.93(7)	108.74(7)	108.2(2)
O(1)–S–O(4)	110.86(10)	110.11(8)	110.28(1)	109.33(11)	109.50(11)	109.59(11)	111.3(4)
H(13)–N(1)–H(14)	101(4)	93(4)	103(4)	110.2(17)			
H(12)–N(1)–H(13)	111(2)	114(2)	104(3)	107.3(20)			
H(12)–N(1)–H(14)	111(2)	114(2)	104(3)	105.9(16)			
H(11)–N(1)–H(13)	112(2)	116(2)	113(3)	111.2(21)			
H(11)–N(1)–H(14)	112(2)	116(2)	113(3)	111.5(18)			
H(11)–N(1)–H(12)	108(3)	102(3)	115(6)	110.3(19)			
H(23)–N(2)–H(24)	107(3)	83(3)	99(4)	110.8(20)			
H(22)–N(2)–H(23)	103(2)	101(2)	101(3)	105.2(22)			
H(22)–N(2)–H(24)	103(2)	101(2)	101(3)	114.0(21)			
H(21)–N(2)–H(23)	111(2)	119(2)	113(3)	106.8(21)			
H(21)–N(2)–H(24)	111(2)	119(2)	113(3)	107.4(20)			
H(21)–N(2)–H(22)	120(2)	121(4)	123(5)	112.1(18)			

samples was determined from N and H analyses with a Carlo Erba microanalyser EA1108, and K and S analyses were carried out using ICP, with a Jobin–Yvon analyser. The values of  $x$  for the single crystals were obtained from x-ray crystal structure refinement.

## 2.2. Thermal analysis

Thermal characterization was carried out using a Perkin–Elmer model DSC-7 differential scanning calorimeter. The sample mass was in the range 20–18 mg. A heating rate of

**Table 4.** Contacts or hydrogen bonds: K, N...O < 3.5 Å for (NH<sub>4</sub>)<sub>2(1-x)</sub>K<sub>2x</sub>SO<sub>4</sub> mixed solid solutions. On the left is the atomic notation for paraelectric phases, and on the right that for ferroelectric phases.

	x = 1.90			x = 0.20			
	298.3 K	234.6 K	174.8 K	298.3 K	232.8 K	183.8 K	
K, N(1)...							
O(1)#0	3.066(2)	3.0662(14)	3.114(6)	3.243(2)	3.245(2)	2.983(2)	O(1)#0
O(1)#1	3.066(2)	3.0662(14)	3.114(6)	3.243(2)	3.245(2)	3.345(2)	O(4)#0
O(2)#0	>3.5	3.429(2)	3.042(9)	3.293(3)	3.267(3)	3.273(2)	O(2)#0
O(2)#3	2.730(2)	2.728(2)	2.799(8)	2.874(2)	2.869(2)	2.966(2)	O(2)#3
O(1)#4	3.095(2)	3.0834(14)	2.974(6)	3.115(2)	3.0940(14)	2.875(2)	O(1)#4
O(1)#5	3.095(2)	3.0834(14)	2.974(6)	3.115(2)	3.0940(14)	3.311(2)	O(4)#4
O(1)#6	2.929(2)	2.922(2)	2.891(6)	3.024(2)	3.013(2)	2.829(2)	O(4)#7
O(3)#7	2.920(2)	2.914(2)	2.944(3)	3.0164(6)	3.0088(8)	3.142(3)	O(3)#7
O(1)#8	2.929(2)	2.922(2)	2.891(6)	3.024(2)	3.013(2)	3.374(2)	O(1)#9
O(3)#9	2.920(2)	2.914(2)	2.944(3)	3.0164(6)	3.0088(8)	2.875(3)	O(3)#9
O(3)#5	3.216(2)	3.202(2)	> 3.5	> 3.5	> 3.5	> 3.5	O(3)#5
N, K(2)...							
O(3)#0	2.731(2)	2.727(2)	2.700(8)	3.381(3)	3.345(3)	3.206(2)	O(2)#0
O(2)#0	2.940(2)	2.930(2)	3.221(9)	2.819(2)	2.763(3)	2.813(2)	O(3)#0
O(1)#10	2.7461(14)	2.7403(13)	2.840(5)	2.9031(12)	2.9114(13)	3.080(2)	O(4)#10
O(1)#11	2.7461(14)	2.7403(13)	2.840(5)	2.9031(12)	2.9114(13)	2.844(2)	O(1)#11
O(3)#12	2.789(2)	2.784(2)	2.829(7)	2.930(2)	2.963(2)	2.982(2)	O(3)#12
O(1)#13	2.819(2)	2.809(2)	2.869(6)	2.9795(13)	2.9794(12)	2.827(2)	O(4)#14
O(2)#14	3.142(2)	3.134(2)	3.040(4)	3.1654(9)	3.1401(10)	3.403(3)	O(2)#14
O(1)#15	2.819(2)	2.8088(14)	2.869(6)	2.9795(13)	2.9794(12)	3.181(2)	O(1)#15
O(2)#16	3.142(2)	3.134(2)	3.40(4)	3.1654(9)	3.1401(10)	2.917(3)	O(2)#16
Symmetry matrices							
#0	x, y, z	#1	x, y, -z + 1/2				
#2	x + 1/2, -y + 1/2, z	#3	x + 1/2, -y + 1/2, -z + 1/2				
#4	x - 1/2, -y + 1/2, z	#5	x - 1/2, -y + 1/2, -z + 1/2				
#6	-x + 1/2, y - 1/2, -z	#7	-x + 1/2, y - 1/2, z - 1/2				
#8	-x + 1/2, y - 1/2, -z + 1	#9	-x + 1/2, y - 1/2, +z + 1/2				
#10	-x + 1/2, y + 1/2, -z	#11	-x + 1/2, y + 1/2, z + 1/2				
#12	x - 1/2, -y + 1/2 + 1, z	#13	-x, -y + 1, -z				
#14	-x, -y + 1, z - 1/2	#15	-x, -y + 1, -z + 1				
#16	-x, -y + 1, z + 1/2						

5 K min<sup>-1</sup> and a total scale sensitivity of 0.4 mW were used. The measurements were carried out during the warming process. The temperature range was 293.3–173.0 K.

### 2.3. X-ray powder diffraction

Powder diffraction data were collected with a Siemens D500 automated diffractometer at different temperatures, using Cu K $\alpha$  radiation and a secondary monochromator. Two processes were carried out. The first process was cooling from 298 to 183 K with a cooling rate of 5 K min<sup>-1</sup>, and the sample was left for 5 min at the measuring temperature, in order to stabilize the equipment and the sample. Measurements were taken at 298.0(1), 243.0(1),

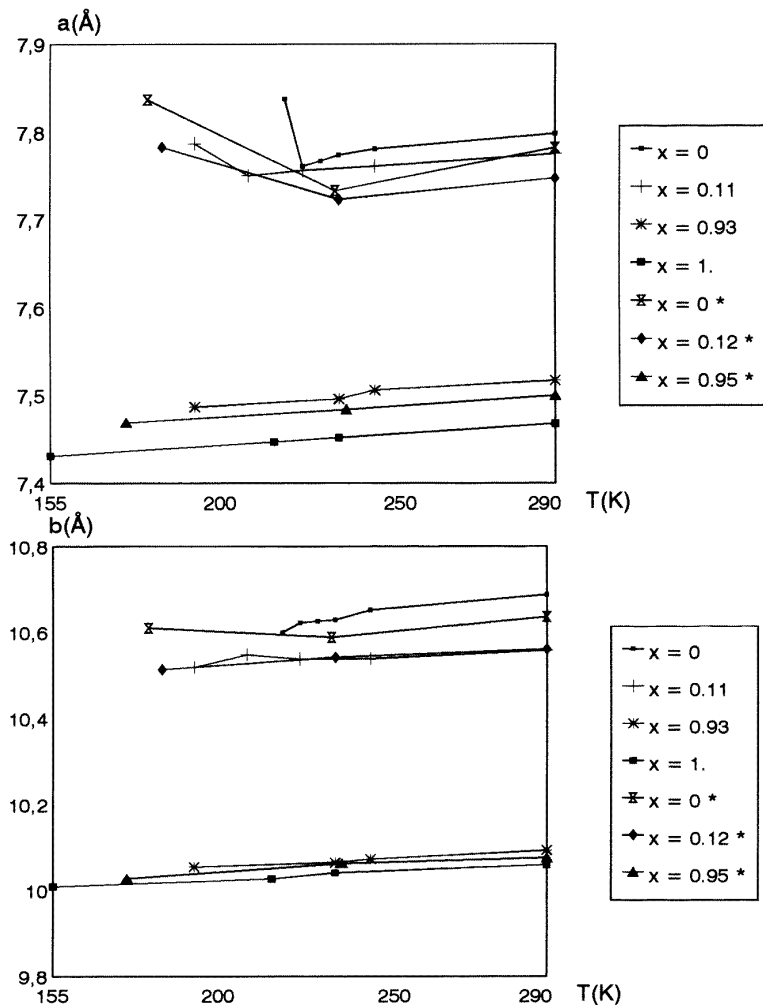


**Figure 1.** Variation in the cell parameters with the temperature according to the value of  $x$ . Values with asterisks in the key are from single-crystal samples; the remaining values are data from powder samples.

**Table 5.** Occupancy factors for N(1) and N(2) sites at 298.3 K in  $(NH_4)_{2(1-x)}K_xSO_4$  mixed crystals. These values remain fixed when the temperature varies.

	Occupancy factor					
	$x = 0$	$x = 0.20$	$x = 0.62$ [10]	$x = 1.40$ [10]	$x = 1.90$	$x = 1$
N(1)	1	0.962(3)	0.85(7)	0.53(5)	0.104(3)	0
K(1)	0	0.038(3)	0.15(7)	0.47(5)	0.896(3)	1
N(2)	1	0.835(3)	0.53(1)	0.08(5)	0	0
K(2)	0	0.165(3)	0.47(1)	0.92(5)	1	1

233.0(2), 228.0(2), 223.0(2) and 218.0(2) K. The step size was 0.025, the time of the step



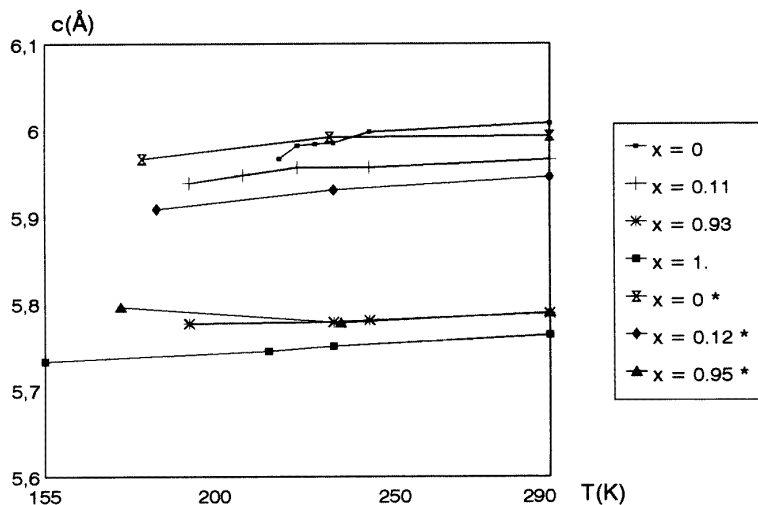


Figure 1. (Continued)

10 s and the  $2\theta$  range  $15\text{--}60^\circ$ . From the end members of the mixed crystals, indexation was carried out and the cell parameters were refined with the CELREF computer program [14]. The second process was cooling from  $220.5(1)$  to  $215.5(1)$  K followed by warming in the same temperature range. The  $2\theta$  range was  $22\text{--}23.45^\circ$ , which is the zone where the (200) reflection occurs. This reflection was selected because it has the largest displacement during the transition.

#### 2.4. X-ray structure determination

A similar method was followed in all crystal structure determinations. Diffraction data were collected on an Enraf–Nonius CAD4 automated diffractometer equipped with a graphite monochromator. The  $\omega$ – $\theta$  scan technique was used to record the intensities. Scan widths were calculated as  $A + B \tan \theta$ , where  $A$  is estimated from the mosaicity of the crystal and  $B$  allows for the increase in peak width due to  $\text{Mo K}\alpha_1$ – $\text{K}\alpha_2$  splitting.

Details of the structure determination are listed in table 1. The unit-cell parameters were obtained by a least-squares fit to the automatically centred settings from 25 reflections ( $12^\circ < 2\theta < 21^\circ$ ). The intensities from three control reflections for each measurement showed no significant fluctuation during the data collection. Intensity data for all structures were corrected for Lorentz and polarization effects, as well as for anomalous dispersion effects. Absorption corrections were not applied.

The structure of  $(\text{NH}_4)_2\text{SO}_4$  was solved by direct methods using the SHELXS computer program [15]. The structures were refined by the full-matrix least-squares method from the data on  $(\text{NH}_4)_2\text{SO}_4$ , using the SHELX-93 computer program [16]. The function minimized was  $w \parallel |F_o|^2 - |F_c|^2 \parallel^2$ , where the weighting scheme was  $w = [\sigma^2(I) + (k_1 P)^2 + k_2 P]^{-1}$  and  $P = (|F_o|^2 + 2|F_c|^2)/3$ . The values of  $k_1$  and  $k_2$  were computed in order to optimize the final  $R$ -value. All hydrogen atoms of rich structures at low K concentrations were obtained from a difference synthesis. The occupancy factors for ammonium and potassium ion in the mixed crystals were refined independently for each site.

**Table 6.** Moments of inertia of the  $SO_4^{2-}$  ion with the direction cosines referenced to Cartesian axes and the librational principal values with the direction cosines referenced to inertial axes.

<i>T</i> (K)	Axis 1				Axis 2				Axis 3			
	Value	Direction cosines			Value	Direction cosines			Value	Direction cosines		
Moments of inertia												
$(NH_4)_2SO_4$												
298.3	93.0	0.73	-0.68	0.00	91.1	0.68	0.73	0.00	91.0	0.00	0.00	1.00
231.8	93.0	0.80	-0.59	0.00	91.3	0.59	0.80	0.00	90.6	0.00	0.00	1.00
173.3	94.2	0.75	0.27	-0.59	92.4	-0.53	0.77	-0.33	91.7	0.36	0.57	0.73
$(NH_4)_{1.8}K_{0.2}SO_4$												
298.3	92.7	0.85	-0.53	0.00	91.2	0.53	0.85	0.00	91.2	0.00	0.00	1.00
232.8	92.9	0.85	-0.53	0.00	91.1	0.53	0.85	0.00	91.3	0.00	0.00	1.00
183.8	93.5	0.92	-0.35	-0.15	92.3	0.37	0.92	0.14	92.8	0.09	-0.19	0.98
$(NH_4)_{0.1}K_{1.9}SO_4$												
298.3	92.7	0.63	-0.78	0.00	92.4	0.78	0.63	0.00	92.2	0.00	0.00	1.00
234.6	93.3	0.64	-0.77	0.00	92.6	0.77	0.63	0.00	92.3	0.00	0.00	1.00
174.8	86.0	0.50	-0.87	0.00	84.0	0.86	0.50	0.00	82.4	0.00	0.00	1.00
$K_2SO_4$												
298.3	92.5	0.75	-0.65	0.00	92.0	0.65	0.75	0.00	91.8	0.00	0.00	1.00
$Rb_2SO_4$												
298.3	93.3	0.57	-0.81	0.00	92.5	0.81	0.57	0.00	92.7	0.00	0.00	1.00
$Cs_2SO_4$												
298.3	93.1	0.38	-0.92	0.00	92.4	0.92	0.38	0.00	92.8	0.00	0.00	1.00
Librational tensors												
298.3	7.3	0.99	0.01	0.00	6.9	-0.01	0.99	0.00	5.6	0.00	0.00	1.00
231.8	7.7	0.96	0.26	0.00	6.5	-0.26	0.96	0.00	7.5	0.00	0.00	1.00
173.3	6.8	0.93	0.25	-0.23	4.4	-0.31	0.91	-0.24	3.4	0.15	0.29	0.94
$(NH_4)_{1.8}K_{0.2}SO_4$												
298.3	7.5	1.00	0.00	0.00	6.9	0.00	1.00	0.00	8.6	0.00	0.00	1.00
232.8	7.2	1.00	0.00	0.00	6.5	0.00	1.00	0.00	7.5	0.00	0.00	1.00
183.8	4.3	0.88	0.46	-0.08	5.6	-0.43	0.87	0.23	5.1	0.18	-0.17	0.97
$(NH_4)_{0.1}K_{1.9}SO_4$												
298.3	6.3	0.99	-0.12	0.00	4.6	0.12	0.99	0.00	5.6	0.00	0.00	1.00
234.6	5.5	0.97	-0.20	0.00	4.3	0.20	0.97	0.00	5.2	0.00	0.00	1.00
174.8	7.8	0.72	0.69	0.00	6.3	-0.69	0.72	0.00	7.5	0.00	0.00	1.00
$K_2SO_4$												
298.3	5.4	0.92	0.38	0.00	4.2	-0.38	0.92	0.00	3.6	0.00	0.00	1.00
$Rb_2SO_4$												
298.3	5.9	1.00	0.00	0.00	4.7	0.00	1.00	0.00	4.6	0.00	0.00	1.00
$Cs_2SO_4$												
298.3	5.9	1.00	0.00	0.00	4.6	0.00	1.00	0.00	5.2	0.00	0.00	1.00

### 3. Results and discussion

#### 3.1. Thermal analyses

$(NH_4)_2SO_4$  shows a transition at 223.2 K (onset temperature) with  $\Delta H = 0.090 \text{ J mol}^{-1}$ , while these values are 205.5 K and  $0.025 \text{ J mol}^{-1}$  for  $(NH_4)_{1.76}K_{0.24}SO_4$ . No transition

was observed for  $(\text{NH}_4)_{0.1}\text{K}_{1.9}\text{SO}_4$ . If we assume an ideal solution behaviour for these solutions,  $\Delta H(x) = \Delta H(0) - kx$ , where  $k = [\Delta H(0) - \Delta H(0.24)]/0.24$ . The transition must disappear at  $x = 0.34$ .

### 3.2. X-ray powder diffraction

The comparison between the position of the (200) reflection during the cooling and the warming processes does not show a thermal hysteresis for  $(\text{NH}_4)_{2-x}\text{K}_x\text{SO}_4$  for  $x = 0$  and 0.20; so the ferroelectric–paraelectric transition is a second-order transition, which agrees with the results of dielectric measurements [2, 17] and Raman spectroscopy [6].

Cell parameters were refined using all identified maxima (from 20 to 35 reflections). Figure 1 shows the obtained values which are compared with those from single-crystal diffractometry. The parameter  $a$  increases abruptly after the Curie temperature for ammonium-rich samples and it depends on the composition of the sample, while the transition is not observed in potassium-rich samples, which agrees with the DSC results.

### 3.3. X-ray crystal structure

The structures are described as follows. The atomic coordinates and temperature coefficients are listed in table 2. Selected interionic bond lengths and angles are listed in table 3.

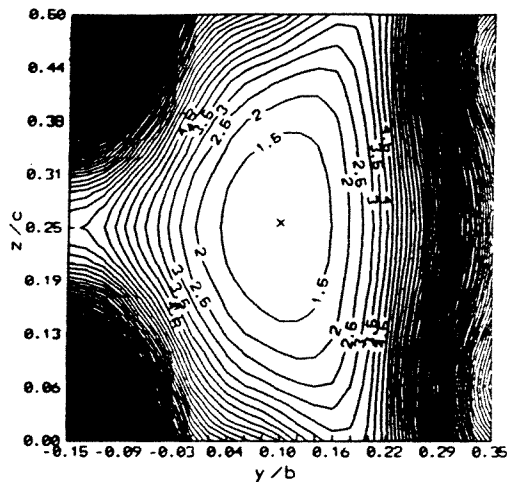
The S–O bond lengths are not equivalent; S–O(2) (the average value for different temperatures is 1.460 Å for  $x = 0.05$  and 1.456 Å for  $x = 0.95$ ) is the shortest; therefore the electronic delocalization in the  $\text{SO}_4^{2-}$  ion is not perfect and there is a lower single-bond character in the S–O(2) bond than in the remaining S–O bonds. According to this result the effective negative charge of O(2) is lower than the remaining O atoms, which is correlated with the average O...N hydrogen bond length for each atom: 3.107 Å for O(2); 3.003 Å for O(1); 2.931 Å for O(3). This asymmetric behaviour of the  $\text{SO}_4$  ion was suggested by Iqbal and Christie [6] from Raman results and it has also been observed for  $\text{K}_2\text{SeO}_4$  [18] but not for  $(\text{NH}_4)_2\text{BeF}_4$  [13].

The thermal coefficients of N(1) and N(2) atoms for  $x = 0.20$  as well as those obtained by Schlemper and Hamilton [19] for  $x = 0$  do not suggest disorder in their localization as was assumed by Hasebe [20] and agree with the comments of Hamilton [21]. At room temperature the  $\text{NH}_4$  ions show a distorted tetragonal coordination (bond angles of between 86 and 120°). This is due to the different number of hydrogen bonds that occur for each hydrogen atom and to the hydrogen bond scheme. This result agrees with the conclusions of Iqbal and Christie [6] from spectroscopy data.

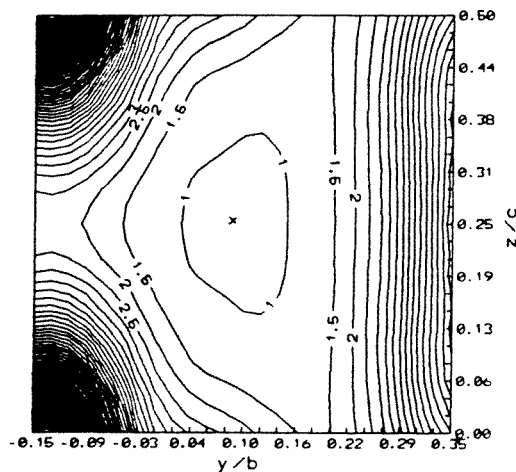
The replacement of  $\text{NH}_4$  by K ions produces a shortening of the average cation–anion lengths (table 4). Using the structure of  $(\text{NH}_4)_2\text{SO}_4$  as the reference [19] and the position of the S atom as the origin, the N(1) site is displaced 0.07 Å along the  $a$  axis for  $x = 0.20$  and 0.10 Å along the  $b$  axis for  $x = 1.90$ , while the N(2) site is displaced 0.13 Å along the  $a$  axis for  $x = 0.20$  and 0.35 Å along the  $[1\bar{1}0]$  direction for  $x = 1.90$ . This N-site displacement is combined with the clockwise rotation of the  $\text{SO}_4^{2-}$  ion around the  $c$  axis (1.6° for  $x = 0.20$  and 9.8° for  $x = 1.90$ ). This explains why the N(1) site is hydrogen bonded to two O(2) atoms for  $x = 0.20$  and only one O(2) atom for  $x = 1.90$ .

Table 5 shows the occupancy factors of ammonium and potassium ions in each anion site. The replacement is not random. The potassium ion, which has the smaller radius, preferentially occupies the smallest hole.

The main structural differences in the paraelectric phase of  $(\text{NH}_4)_{2-x}\text{K}_x\text{SO}_4$  at different temperatures is the counter-clockwise rotation of the  $\text{SO}_4^{2-}$  ion around the  $c$  axis for  $x = 0$



(a)

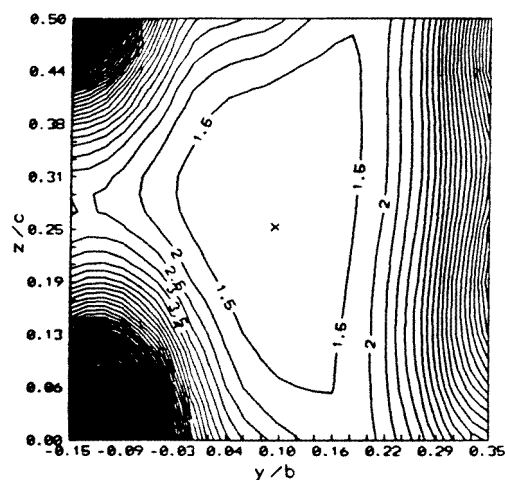


(b)

**Figure 2.** Map parallel to (010) plane of the sum of bond valence in the N(1) site: (a) for  $(NH_4)_{0.1}K_{1.9}SO_4$  at 274.6 K and  $y = 0.0897$ ; (b) for  $(NH_4)_{1.8}K_{0.2}SO_4$  at 232.8 K and  $y = 0.0966$ ; (c) for  $(NH_4)_{1.8}K_{0.2}SO_4$  at 183.8 K and  $y = 0.1042$ .

and  $x = 0.20$  ( $1.0^\circ$  at 231.5 K for  $x = 0$  and  $0.7^\circ$  at 232.8 K for  $x = 0.20$  with respect to the 298 K position), while it is not produced for  $x = 1.90$ , where only a shortening of all K...O lengths occurs.

A study on the moments of inertia and librational tensor of the  $SO_4^{2-}$  ion has been carried out. We used the EKRT computer program [22], where the thermal coefficients of the sulphate ion are equal to  $GL + HS + T$ ;  $T$  is the translational tensor,  $L$  and  $S$  are the



(c)

Figure 2. (Continued)

librational tensors, and  $G$  and  $H$  are the geometrical matrices which connect the atomic positions and the mass centre. The function minimized was  $\Sigma \sigma^{-1} (U_c - U_o)^2$ . The study has been carried out on  $(\text{NH}_4)_2\text{SO}_4$  at three different temperatures; the values for 298.3 and 173.3 K were from the work of Schlemper and Hamilton [19]. The two mixed crystals of this paper and the three sulphates  $\text{K}_2\text{SO}_4$  [23],  $\text{RbSO}_4$  and  $\text{Cs}_2\text{SO}_4$  [24], which do not show the paraelectric–ferroelectric transition, were studied. The  $\text{SO}_4^{2-}$  ion was assumed as a rigid ion. The results are given in table 6, where it is observed that the moment of inertia is almost constant, which justifies the assumption that it is a rigid body. Differences in the moment of inertia are observed only for the structure with  $x = 1.90$  at 174.8 K, but this is attributed to the low accuracy of its crystal structure determination. The cosine director components confirm the  $\text{SO}_4^{2-}$  rotation around the  $b$  axis when  $x$  increases.

The paraelectric phases in the paraelectric–ferroelectric transition show higher librational principal values than those observed in the remaining compounds. The values for compounds with the transition are similar to those observed for  $\text{K}_2\text{SeO}_4$  [18]; so this must be a condition for producing the transition in these compounds. We have computed the librational frequency along the  $c$  axis, using the equation

$$v^2 = kT/4\pi^2 I_o L_o^2 c^2$$

obtaining the values 80.17, 92.81, 106.23, 113.75 and 177.57  $\text{cm}^{-1}$  for  $x = 0, 0.20, 1.40, 1.90$  and 1, respectively. (These values are 135.11 and 138.10 for rubidium and caesium sulphates, respectively). All this suggests that the transition from the paraelectric to the ferroelectric phase is a displacive transition with a ‘pseudo-soft mode’.

In order to confirm this, we have computed a density map of the sum of bond valences in the N(1) site according to the Brown [25] theory. It is observed (figure 2) that the anisotropy and the size of the hole vary according to the value of  $x$ . The smallest size of the hole is in the direction of the  $a$  axis, which is parallel to the  $\text{O}(2)\#3 \dots \text{N}(1)$  hydrogen bond. The hydrogen bond of N(1) has the shortest length. Therefore, this direction is assigned as the strain direction necessary to produce the transition. The strain disappears after the

transition, increasing the value of parameter  $a$  (figure 1). The largest size of the hole is in the  $c$  axis direction. So the transition from the paraelectric to the ferroelectric phase is produced by a displacement of N(1) along the  $c$  axis in order to increase the valence sum according to the distortion theorem of Brown. The hole for the ferroelectric phase shows a displacement of N(1) along the  $c$  axis, breaking the mirror-plane symmetry and does not show an irregular form which could suggest disorder in the N(1) localization.

We have indicated that the transition is displacive with a 'pseudo-soft mode', because the hydrogen bonds in the mixed crystal  $(\text{NH}_4)_{2(1-x)}\text{K}_{2x}\text{SO}_4$  are stronger than those observed in  $(\text{NH}_4)_2\text{BeF}_4$ . (The average value in the sulphate derivative is equal to 2.94 Å, while it is 3.15 Å for the tetrafluoroberyllate compound. The shortest bonds are 2.73 Å in the first and 2.93 Å in the second compound.) The hydrogen bonds are not broken during the transition; so the soft mode is not produced during the transition.

### Acknowledgments

A fellowship from the Ministerio de Educación y Ciencia (DGICYT-MAT95-02180) is gratefully acknowledged. Two of us (C G-S and C R-P) thank the Consejería de Educación del Gobierno Canario (208/94) for financial support.

### References

- [1] Mattias B T and Remeika J P 1956 *Phys. Rev.* **103** 262
- [2] Hoshino S, Vedam K, Okaya Y and Pepinsky R 1958 *Phys. Rev.* **112** 405
- [3] Onodera A, Fujishita H and Shiozaki Y 1978 *Solid State Commun.* **27** 243
- [4] O'Really D E and Tsang T 1967 *J. Chem. Phys.* **46** 1291
- [5] Sawada A, Takagi Y and Ishibashi Y 1973 *J. Phys. Soc. Japan* **34** 748
- [6] Iqbal Z and Christoe C W 1976 *Solid State Commun.* **18** 269
- [7] Nordland T J, O'Reilly D E and Peterson E M 1976 *J. Chem. Phys.* **64** 1838
- [8] Sawada A, Ohya S, Ishibashi Y and Takagi Y 1975 *J. Phys. Soc. Japan* **38** 1408
- [9] Kasahara M, Sasakawa K and Tatsuzaki I 1975 *J. Phys. Soc. Japan* **39** 1022
- [10] Shiozaki Y, Koh S and Sawaguchi E 1977 *J. Phys. Soc. Japan* **43** 721
- [11] Martínez-Sarrión M L, Rodríguez-Clemente A, Mestres L, Ventura B and Bocanegra E H 1995 *Ferroelectrics* **166** 3
- [12] Martínez-Sarrión M L, Rodríguez-Clemente A, Mestres L, Lozano A and Solans X 1991 *Ferroelectrics* **120** 271
- [13] González-Silgo C, Ruiz-Pérez C, Solans X, Martínez-Sarrión M L, Mestres L, Rodríguez A and Bocanegra E 1996 *Ferroelectrics* **175** 207
- [14] Laugier J and Filhol A 1978 *Program CELREF* (Grenoble: Institute Langevin)
- [15] Sheldrick G M 1990 *Acta Crystallogr. A* **46** 467
- [16] Sheldrick G M 1994 *SHELXL* (Göttingen: University of Göttingen)
- [17] Unruh H G 1970 *Solid State Commun.* **8** 1951
- [18] González-Silgo C, Solans X, Ruiz-Pérez C, Martínez-Sarrión M L and Mestres L 1996 *Ferroelectrics* **177** 191
- [19] Schlemper E O and Hamilton W C 1966 *J. Phys. C: Solid State Phys.* **44** 4498
- [20] Hasebe K 1981 *J. Phys. Soc. Japan* **50** 1266
- [21] Hamilton W C 1969 *J. Chem. Phys.* **50** 2275
- [22] Craven B M, He X and Weber H P 1992 *Program EKRT* (Pittsburgh, PA: University of Pittsburg)
- [23] McGinnety J A 1972 *Acta Crystallogr. B* **28** 2845
- [24] Weber H J, Schulz M, Scmitz S, Gramzin J and Siegert H 1989 *J. Phys.: Condens. Matter* **1** 8543
- [25] Brown I D 1992 *Acta Crystallogr. B* **48** 553